The very strong role played by the apolar environment is also evident in a comparison of 25 and 10% laurylated polyethylenimines (A and C, respectively, in Table I). The catalytic constant k_2, reflecting the effect of polymer environment on the transition state, drops by a factor of 5 in the less apolar environment.

All of the polymers show marked catalytic effects on the decarboxylation in the water solvent. In the polymer environment the intrinsic first-order rate constant, k_2, can be 10^3-fold greater than the pseudo-first-order rate constant in the aqueous solvent alone (B and E, respectively, in Table I). Furthermore, the polymer is an effective catalyst at concentrations of the order of 10^{-6} M, corresponding to catalytic site concentrations of about 10^{-4} M. This means that the decarboxylation rate can be enhanced more than 1000 times by addition of 5×10^{-6} M polymer to the aqueous solution. In contrast, for micellar systems, the maximum enhancement reported is at best 100-fold.[2]

Comparison of the catalytic effectiveness of the polyethylenimines on the two different substrates, nitrobenzisoxazolecarboxylate and cyanophenylacetic acid, is hampered by our inability to obtain data at high concentration of polymer, i.e., $C_0 \gg S_0$. Nevertheless, it is clear from the few experiments at $C_0 \sim S_0$ that k_2 for the cyanophenylacetic acid must be above 6×10^{-4} s^{-1}. The corresponding constant for nitrobenzisoxazolecarboxylate is 39.2×10^{-4} s^{-1}, at most, therefore, a factor of perhaps 6 greater. Since the spontaneous rate for cyanophenylacetate is some threefold slower than that for the benzisoxazole, we can see that the effect of the polymer environment on the stabilization of the transition state is approximately the same for each substrate. On the other hand, the binding affinity of the polymer for cyanophenylacetate, as measured by K_M^{-1}, is about tenfold weaker. This weaker affinity for the smaller substrate is not surprising in view of similar observations with other aromatic molecules and polyethylenimines.[4,16]

Thus it is evident that the modified polyethylenimines provide a matrix for achieving homogeneous catalysis of decarboxylation of anionic substrates in an aqueous environment. For nitrobenzisoxazolecarboxylate, as has been demonstrated by Kemp and Paul,[1] the transition state is a charge-delocalized anionic structure, stabilized in aprotic solvents by dispersion interactions. Clearly, the modified polyethylenimines also provide solvation features that stabilize the anionic transition structure in the state with particularly sensitive bonds.

The modified polyethylenimines described herein are only a few of many possibilities. The matrix of this polymer provides a framework for attachment of a variety of different types of apolar or polar (protic and aprotic) groups. Thus a wide range of local environments can be created on this macromolecular water-soluble catalyst. Large solvent effects have been observed in kinetic studies of many reactions involving anions.[1,17] Suitable derivatives of polyethylenimine should manifest interesting effects in many of these reactions.

Acknowledgment. This investigation was supported in part by grants from the National Science Foundation (No. BMS72-02204) and from the National Institutes of General Medical Sciences, U.S. Public Health Service (No. GM09280).

References and Notes

(1) D. S. Kemp and K. Paul, *J. Am. Chem. Soc.*, **92**, 2553 (1970); **97**, 7305 (1975).
(2) C. A. Bunton and M. Minch, *Tetrahedron Lett.*, 3881 (1970).
(3) J. Smid, S. Shah, L. Wong, and J. Hurley, *J. Am. Chem. Soc.*, **97**, 5932 (1975).
(4) I. M. Klotz, G. P. Royer, and A. R. Sloniewsky, *Biochemistry*, **8**, 4752 (1969).
(5) I. M. Klotz, G. P. Royer, and I. S. Scarpa, *Proc. Natl. Acad. Sci. U.S.A.*, **68**, 263 (1971).
(6) I. S. Scarpa, H. C. Kiefer, and I. M. Klotz, *Intra-Sci. Chem. Rep.*, **8**, 45 (1974).
(7) T. W. Johnson and I. M. Klotz, *Macromolecules*, **7**, 149 (1974).
(8) H. Z. Sommez, H. I. Lipp, and L. L. Jackson, *J. Org. Chem.*, **36**, 824 (1971).
(9) S. S. Sabnis and M. V. Shirsat, *J. Sci. Ind. Res.*, **178**, 451 (1958).
(10) W. Borsche, *Justus Liebigs Ann. Chem.*, **390**, 1 (1912).
(11) H. Lindemann and H. Cissée, *Justus Liebigs Ann. Chem.*, **469**, 44 (1929).
(12) T. S. Straub and M. L. Bender, *J. Am. Chem. Soc.*, **94**, 8875 (1972).
(13) J. C. Hessler, *Am. Chem. J.*, **32**, 119 (1904).
(14) L. Michaelis and M. L. Menten, *Biochem. Z.*, **49**, 333 (1913).
(15) A. Thomson, *J. Chem. Soc. B*, 1198 (1970).
(16) T. W. Johnson and I. M. Klotz, *Biopolymers*, **13**, 791 (1974).
(17) A. J. Parker, *Adv. Phys. Org. Chem.*, **5**, 173 (1967); *Chem. Rev.*, **69**, 1 (1969).

Substituent Effects on the Solution Conformation of Rifamycin S

M. F. Dampier, C-W. Chen, and H. W. Whitlock, Jr.*

Contribution from the Department of Chemistry, University of Wisconsin, Madison, Wisconsin 53706. *Received February 18, 1976*

Abstract: The synthesis of several new rifamycin derivatives is presented. Correlations of their NMR spectra indicate that C-3 substitution effects the overall conformation of the ansa bridge. These conformational changes probably effect the enzyme inhibitory activity of these derivatives.

We have previously shown that the in vitro effectiveness of 3-substituted derivatives of rifamycin S as inhibitors of RNA synthesis by *Escherichia coli* DNA dependent RNA polymerase correlates with the electronegativity of the substituents, in particular with Hammett's σ_p.[1] These data, coupled with inhibition reversibility for the weaker inhibitors, were taken to implicate charge-transfer complexes (or some hydrophobic equivalent) in the inhibition interactions between the rifamycins and RNA polymerase. Since this conclusion is based on the assumption that the various rifamycin derivatives (Figure 1) possess similar conformations of the ansa bridge relative to the aromatic ring, we felt that this should be tested by carrying out a detailed high-field proton NMR examination of them. The results of this work are reported below, our main conclusion being that although the ansa bridge is relatively rigid, it appears to rock as a unit about pivot points at each end

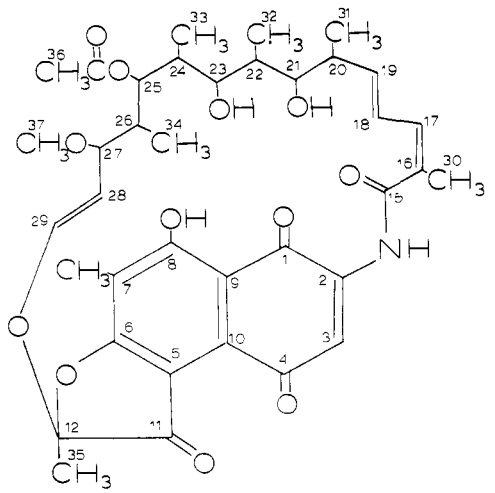

Figure 1. Structure and numbering convention used for the rifamycin derivatives.

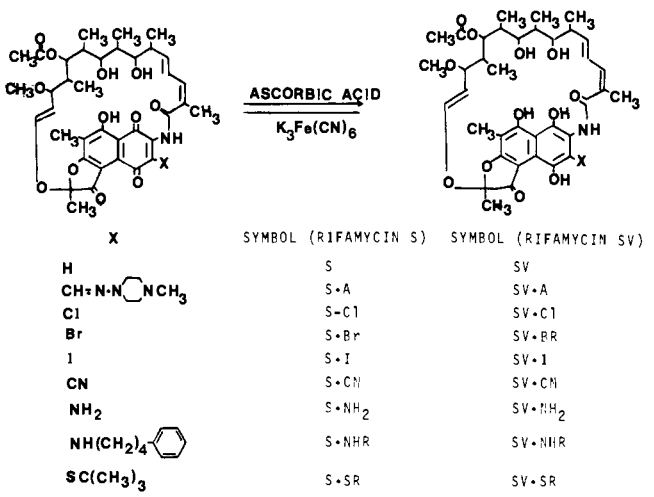

X	SYMBOL (RIFAMYCIN S)	SYMBOL (RIFAMYCIN SV)
H	S	SV
CH=N-N◯NCH$_3$	S-A	SV-A
Cl	S-Cl	SV-Cl
Br	S-Br	SV-BR
I	S-I	SV-I
CN	S-CN	SV-CN
NH_2	S-NH_2	SV-NH_2
NH(CH$_2$)$_4$◯	S-NHR	SV-NHR
SC(CH$_3$)$_3$	S-SR	SV-SR

Figure 2. List and position of substitution of the rifamycin S and rifamycin SV derivatives.

in a substituent-dependent manner. As some of these compounds are both quite active biologically and quite tricky to prepare, we report their synthesis in some detail.

Experimental Section

General Procedure. Silica gel PF-254 (1.5–2.0 mm, Brinkman, Des Plaines, Ill.) was used for preparative chromatography, and silica gel type H was used for column chromatography. Prepared plates, Silplate (0.25 mm) F-22, were used for the R_f determinations. Mass spectra were obtained on an AEI MS-902 mass spectrometer. Proton NMR spectra were recorded on a Bruker WH-270 MHz spectrometer in the Fourier transform mode, operating at a probe temperature of 21 °C. Chemical shifts are reported relative to internal tetramethylsilane even though chloroform (δ 7.25) was used as an internal standard. The concentration of all the samples was 1–2% (w/v). In all cases the structures assigned are consistent with the complete assignment of the NMR spectra.

Rifamycin S (S). Rifamycin SV (Calbiochem) was oxidized to rifamycin S using 1 mol equiv of $K_3Fe(CN)_6$ in pyridine at 0 °C (Figure 2).

3-Bromorifamycin S (S-Br). To a stirred solution of rifamycin SV (735 mg, 1.06 mmol) in 10 ml of absolute ethanol at 4 °C was added in one portion pyridinium bromide perbromide (614 mg, 1.90 mmol). After stirring for 30 min at 4 °C, the reaction mixture was diluted with 100 ml of distilled water and the aqueous layer was extracted with three 75-ml portions of chloroform. The combined organic extracts were washed with 100 ml of 5% acetic acid and then with three 100-ml portions of water. The organic phase was removed, dried over anhydrous sodium sulfate, and concentrated to 2 ml. This was applied to a 2.5 × 85 cm silica gel column which was then eluted with a 2-l. linear gradient of chloroform to 5% methanol–chloroform. The fractions containing the 3-bromorifamycin S were located by TLC [R_f 0.4 (2.5% methanol–chloroform)] and the fractions pooled. The chloroform–methanol solution was washed with 5% acetic acid (the compound is eluted as a metal salt) and three times with water, dried over anhydrous Na_2SO_4, and concentrated in vacuo to yield 230 mg (30%) 3-bromorifamycin S: mp 154–157 °C; R_f 0.53 (ethyl acetate); liquid chromatography (LC) retention volume [Corasil C-18 (3 mm o.d. × 60 cm); 35% acetonitrile in water; 1 ml/min] 3.5 ml; λ_{max} (MeOH) 401 (4370), 392, 274 (27 500); NMR ($DCCl_3$) see Table I. Anal. Calcd for $C_{37}H_{44}NO_{12}Br$: C, 57.31; H, 5.67; N, 1.81. Found: C, 55.45; H, 5.72; N, 2.4.

3-Chlororifamycin S (S-Cl). To a stirred solution of 270 mg of lithium chloride in 32 ml of acetone was added 122 mg of 3-bromorifamycin S. The reaction was stirred under nitrogen for 24 h and then diluted with 100 ml of chloroform. The chloroform–acetone solution was washed with 2 vol of distilled water and the organic phase was dried over anhydrous Na_2SO_4 and evaporated in vacuo. The 3-chlororifamycin S was purified using preparative thick-layer chromatography (ethyl acetate, R_f 0.6). After isolation from the silica gel, the 3-chlororifamycin S anion was reprotonated and recrystallized as described above to yield 62.1 mg of product: mp 161–163 °C dec; R_f 0.20 (1% methanol in chloroform), 0.40 (2.5% methanol in chloroform), 0.56 (ethyl acetate); LC retention volume (Corasil C-18, 35% acetronitrile–65% water, 1 ml/min) 4.2 ml; λ_{max} (MeOH) 504 (5250), 300, 273 (21 900); NMR ($DCCl_3$) δ 1.748 (3 H, s, CH_3), 12.561 ppm (1 H, s, phenol). Anal. Calcd for $C_{37}H_{44}NO_{12}Cl$: C, 60.80; H, 6.02; N, 1.91. Found: C, 59.17; H, 5.98; N, 1.93.

3-Iodorifamycin S (S-I). *Small* iodine crystals (0.69 mmol, 178 mg) were dissolved in 5 ml of *rapidly stirred* pyridine at 25 °C. Immediately after the iodine crystals dissolved, solid rifamycin SV (0.69 mmol, 481 mg) was added in one portion to the iodine–pyridine reagent. After 30 min the reaction solution was diluted with 50 ml of ethyl acetate and shaken with 100 ml of 20% aqueous $K_3Fe(CN)_6$. The organic phase was washed with 10% acetic acid and then with distilled water until the pH of the aqueous phase was between 6 and 7. The ethyl acetate layer was removed, dried over anhydrous sodium sulfate, and evaporated. The residue (470 mg) containing rifamycin S and 3-iodorifamycin S was purified by silica gel column chromatography as described above to yield 168 mg (37%) of 3-iodorifamycin S: mp 154–156 °C dec; LC retention volume (Corasil C-18, 35% acetonitrile–65% water, 0.8 ml/min) 6.0 ml; λ_{max} (MeOH) 410 (5250), 351 (7410), 274 (30 900); NMR ($DCCl_3$) δ see Table I, the additional absorbances are 1.758 (3 H, s, CH_3) and 12.505 ppm (1 H, s, phenol). Anal. Calcd for $C_{37}H_{44}NO_{12}I$: C, 54.03; H, 5.35; N, 1.70. Found: C, 53.05; H, 5.53; N, 1.52.

3-Cyanorifamycin S (S-CN). Ammonium chloride (1.12 g), potassium cyanide (0.98 g), and rifamycin S (0.318 g) were stirred in 3 ml of freshly distilled dimethylformamide for 15 h at 25 °C. The reaction mixture was diluted with 100 ml of ethyl acetate and the excess potassium cyanide removed by washing with three 100-ml portions of distilled water. The organic phase was stirred with 100 ml of 10% aqueous $K_3Fe(CN)_6$ for 5 min and then worked up as described for 3-iodorifamycin S. The residue (300 mg) was purified by two successive preparative thick-layer chromatography steps using ethyl acetate as a solvent. The 3-cyanorifamycin S was recrystalized from ether with hexane yielding 32.7 mg (10 wt %) of compound: mp 151–153 ° C dec; ir 4.45 μ; R_f 0.20 (2.5% methanol in chloroform), 0.11 (1% methanol in chloroform); λ_{max} (MeOH) 534 (3800), 340 (7240), 272 (19 500); NMR ($DCCl_3$) δ see Table I, compound **1e**, additional absorbances at 1.720 (3 H, s, CH_3) and 12.297 ppm (1 H, br s, phenol). Anal. Calcd for $C_{38}H_{44}N_2O_{12}$: C, 63.26; H, 6.10; N, 3.88. Found: C, 61.51; H, 6.24; N, 3.61.

3-Aminorifamycin S (S-NH_2), 3-(4′-Phenylbutylamino)rifamycin S (S-NHR), and 3-*tert*-Butylmercaptorifamycin S (S-SR). The 3-phenylbutylaminorifamycin S, 3-aminorifamycin S, and 3-*tert*-butylmercaptorifamycin S were synthesized by the addition of the appropriate nucleophile to rifamycin S in *p*-dioxane.

3-Phenylbutylaminorifamycin S: mp 91–92 °C dec; molecular weight of its acetonide, calcd for the 21,23-acetonide ($C_{50}H_{62}N_2O_{12}$) 882.42990, found (P^+) 882.428613; R_f 0.78 (1:1 ether–ethyl acetate); λ_{max} (MeOH) 534 (1470), 370 (6160), 315 (11 750), 262 (25 100); NMR ($DCCl_3$) δ see Table I, plus additional absorbances at δ 1.18 (4 H, s, CH_2), 1.67 (3 H, s, CH_3), 2.54 (2 H, t, J = 6 Hz), 7.08–7.20 (5 H, m, ArH), 14.00 ppm (1 H, s, phenol). Anal. Calcd for

Table I. Chemical Shifts for the Ansa Bridge Protons of 3-Substituted Rifamycin S Derivatives[a]

S·NH$_2$	S-SR	S-Cl	S·Br	S-I	S-CN	S		S	S-CN	S·I	S-Br	S-Cl	S·SR	S·NH$_2$
8.14	8.00	8.05	8.25	8.21	8.53	8.36	H—N							
							C=O							
							C—CH$_3$	2.07	2.04	2.07	2.01	2.07	2.09	2.05
6.26	6.27	6.34	6.30	6.40	6.45	6.01	H—C							
10.7	11	10.7	10.7	10.7		8								
6.38	6.50	6.54	6.62	6.85	6.45	6.34	H—C							
15.0	16	15.5	15.6	15.8	14.2	15								
6.12	5.83	5.98	6.00	6.12	6.02	5.92	H—C							
6.8	6.8	8	7.3	7.1	7.8	7								
						2.28	H—C—CH$_3$	0.87	0.84	0.85	0.78	0.81	0.78	0.85
10	6.3	9.8	8	8.2	9.8	9								
3.67	3.59	3.64	3.69	3.82	3.56	3.58	H—C—OH	3.66	3.53	3.48		~3.50	3.30	3.60
						1								
						1.68	H—C—CH$_3$	0.97	0.95	1.01	0.94	0.97	0.95	1.03
				2?	1	1								
3.02	3.07	3.00	3.00	3.05	3.01	3.01	H—C—OH	3.88	3.81	3.80	3.97	3.92	3.78	3.83
10			7	6.8	8	8								
						1.41	H—C—CH$_3$	0.67	0.68	0.68	0.63	0.69	0.64	0.66
<1	<1	<1	<1	<1	<1	1.5								
4.91	5.00	5.00	4.98	5.04	4.83	4.65	H—C—OAc	2.05	2.04	2.07	2.01	2.07	2.05	2.05
10.7	8.5	10	10	10	8.8	10								
						1.93	H—C—CH$_3$	0.15	0.28	0.10	0.14	0.29	0.36	0.07
		3	3	1?	3.9	3								
3.45	3.36	3.37	3.38	4.05	3.67	3.4	H—C—OMe	3.13	3.10	3.10	3.07	3.07	3.10	3.08
6	6.5	6	5	4.3	6.3	8								
5.10	4.97	5.00	4.98	5.04	5.01	5.09	H—C							
12	12.5	12.2	12.2	12.6	12.5	13								
6.08	6.04	5.95	5.90	5.95	6.08	6.25	H—C							
							O							

[a] Chemical shifts are listed on line with their respective protons in parts per million relative to internal Me_4Si. Coupling constants are listed between the chemical shifts of the coupled protons.

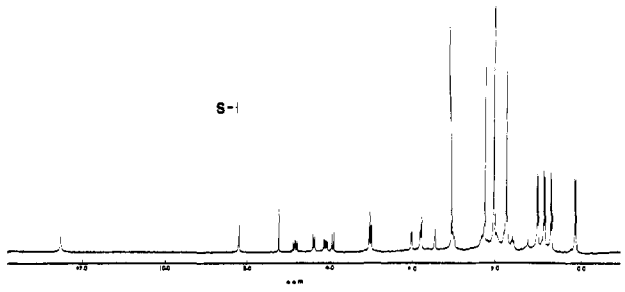

Figure 3. The proton NMR spectrum of 3-iodorifamycin S in chloroform-*d* at 270 MHz.

$C_{47}H_{38}N_2O_{12}$: C, 66.95; H, 6.94; N, 3.23. Found: C, 66.04; H, 7.03; N, 3.13.

3-Aminorifamycin S: mp 171–173 °C (lit.[4] 171–172 °C); R_f 0.42 (ethyl acetate), 0.08 (ether), 0.61 (5% methanol–95% chloroform); λ_{max} (MeOH) 377 (4265), 311 (9120), 264 (20 890); ϵ 377 (3.63), 311 (3.96), 264 (4.32), 218 (4.32); NMR ($DCCl_3$) δ see Table I.

***tert*-Butylmercaptorifamycin S:** mp 154–156 °C dec; R_f 0.431 (ether), 0.57 (ethyl acetate); λ_{max} (MeOH) 330 (4790), 273 (21 900). Anal. Calcd for $C_{41}H_{54}NO_2S$: C, 62.78; H, 6.76; N, 1.78; *m/e* of M^+, 785. Found: C, 62.30; H, 6.78; N, 1.76; M^+ at *m/e* 785.

Synthesis of 3-Substituted Rifamycin SV Derivatives. All of the 3-substituted rifamycin SV compound were synthesized from the appropriate rifamycin S derivative by reduction with 10 mol equiv of ascorbic acid in 66% aqueous methanol for 30 min. The rifamycin SV derivative was obtained by chloroform extraction of the reducing solution.

Results and Discussion

General Features of the Spectra. A typical 270-Hz spectrum, that of 3-iodorifamycins S in chloroform-*d*, is presented in Figure 3. All 49 protons of the molecule are visible and can be assigned with certainty except for the four CH_3–C*H*'s of the ansa bridge; these are partially obscured by the methyl singlets in the 2-ppm region. Coupling patterns were usually sufficiently similar to those of the thoroughly analyzed rifamycin S that assignments could be made by inspection of the spectrum with a high degree of confidence. Selective decoupling and deuterium washout experiments were carried out when needed. Chemical shift concentration effects were absent in chloroform-*d*.[2] The nine methyl groups appear as five distinct singlets and four high-field doublets. In the 3-substituted rifamycin derivatives wherein the ansa bridge has not been ruptured (this study), the high-field methyl doublets are found between 0 and 1 ppm, whereas in the 3-substituted rifamycin SV derivatives these same methyl groups are found at up to ca. −0.5 ppm. In most cases there is good separation between the multiplets in the 5.5–7.0 ppm region which arises from the vinyl protons $C^{17}H$, $c^{18}H$, $C^{19}H$, and $C^{29}H$ (Figures 4 and 5). The absence of the absorption for the aromatic proton normally found at 7.82 ppm in the spectrum of rifamycin S was used as confirming evidence for the position of substitution.

It has been shown previously[2,3,5,6] that the conformation of rifamycin S in solution, as determined by application of the Karplus equation, $J = J_0 \cos^2 \theta$, to vicinal coupling constants, is in good agreement with that found in the solid state for rifamycin B by x-ray methods. Comparison of the coupling constants, or equivalently the derived dihedral angles, allows the following trends to be observed.

(1) Changes in J_{vic} with substituent changes seem to reflect perturbation of one basic conformation of the ansa bridge. Our conclusions (see Figure 6) are consistent with the center portion of the ansa bridge remaining in a relatively static conformation.

(2) Introduction of any substituent at C-3 in rifamycin S leads to marked changes in the dihedral angle about C^{17}–C^{18} and C^{27}–C^{28}. In the former case one observes J_{vic} going from 8 Hz in rifamycin S to 10.8 ± 0.2 Hz in all monosubstituted derivatives, while in the latter case J_{vic} goes from 8 Hz to as low as 4.3 Hz for S-I. While there are other substituent-dependent changes, as a first approximation introduction of any

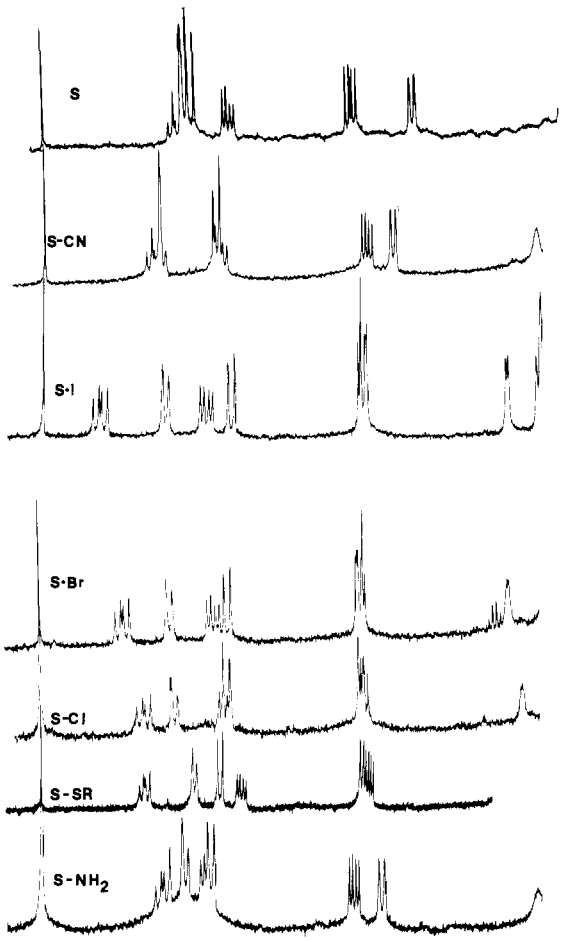

Figure 4. The proton NMR spectra of the vinyl region (4.0–7.6 ppm) for the 3-substituted rifamycin S derivatives: S, rifamycin S; S-CN, 3-cyanorifamycin S; S-I, 3-iodorifamycin S; S-Br, 3-bromorifamycin S; S-Cl, 3-chlororifamycin S; S-SR, 3-*tert*-butylmercaptorifamycin S; S-NH_2, 3-aminorifamycin S.

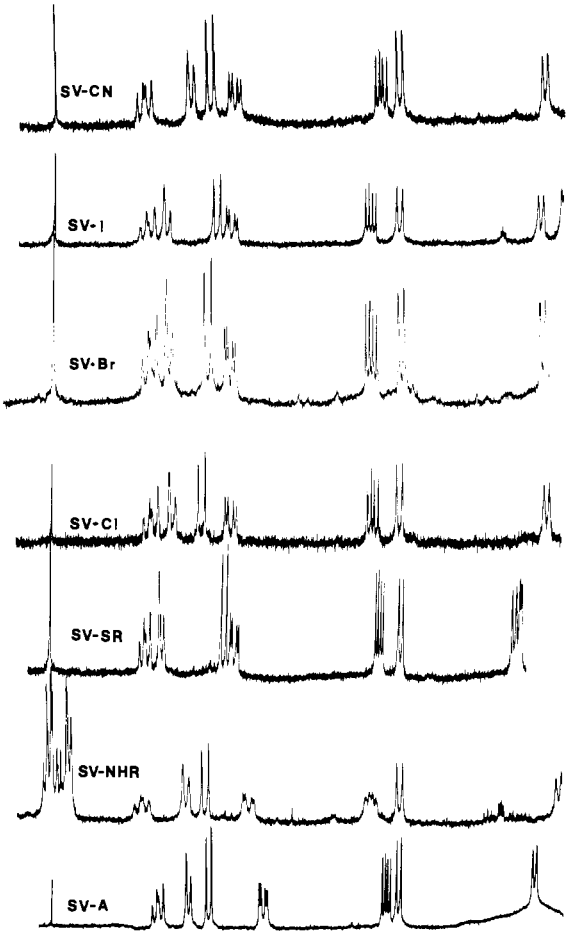

Figure 5. The vinyl portion (4.0–7.5 ppm) of the NMR spectra of the 3-substituted rifamycin SV derivatives: SV-CN, 3-cyanorifamycin SV; SV-I, 3-iodorifamycin SV; SV-Br, 3-bromorifamycin SV; SV-Cl, 3-chlororifamycin SV: SV-SR, 3-*tert*-butylmercaptorifamycin SV; SV-NHR, 3-phenylbutylaminorifamycin SV; and SV-A, rifampicin.

substituent at C-3 results in an overall rocking of the more or less rigid ansa bridge by a angle of ~25–30° about the pivot point C^{17}–C^{18} and 4–18° about C^{27}–C^{28} (Figure 7).

(3) In contrast to rifamycin S, C-3 substituted derivatives of rifamycin SV do not show appreciable changes in J_{vic} for C^{17}–C^{18}, C^{27}–C^{28}, or for any other of the two-carbon units of the ansa bridge (Table II). Rifampicin quinone and rifampicin are indistinguishable from similar S and SV derivatives.

(4) Within the group of C-3 substituted rifamycin S's there are clearly substituent-dependent changes in the conformation of the ansa bridge. Particularly striking is the series S-Cl, S-Br, S-I wherein $J_{C^{27}-C^{28}}$ decreases from 6 Hz for S-Cl to 5 Hz for S-Br to 4.3 Hz for S-I. This is accompanied by a change in chemical shift of the C^{34}-methyl from δ 0.29 for S-Cl to 0.14 for S-Br to 0.10 for S-I. If one ignores resonance effects (this would probably be inappropriate for S-NH_2), one concludes that as the halogen at C^3 gets bigger there is a wiggling of the distal part of the ansa bridge as shown in Figure 6. Again this effect is absent in the SV series. These effects seem to correlate with van der Waals radii or covalent bond lengths as a measure of size (the latter being used in the Figures) but not very well with *A* values. The likely complication of electronic and polarizability effects makes it impossible to distinguish between the importance of the two measures above.

(5) The chemical shifts of the vinyl protons at C^{17} and C^{18} of the rifamycin S derivative [but not rifamycin SV's (see Figure 5)] are substituent dependent. This gives rise to the remarkable qualitative change in the appearance of the vinyl region of the NMR spectra of these molecules (Figure 4). As

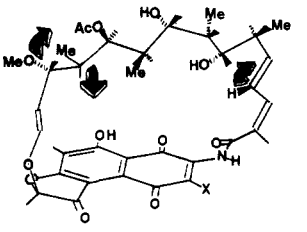

Figure 6. Conformational changes in the rifamycin S ansa bridge as per substituents (see text). The structure is modeled after that in ref 5.

is shown in Figure 8 the chemical shifts of the protons at C^{17} and C^{18} of rifamycin S's correlate with the size of the substituent. We suspect that for the C^{18} proton this dependence reflects the interaction of this proton with the amide carbonyl, the rocking of the ring corresponding to a twist about the C^{15}–C^{16} bond. We cannot make definite statements about the slopes of these lines, nor can we tell whether the twist about the C^{15}–C^{16} bond is a bending back or a bending forward; there are obviously different factors at work which effect the chemical shifts of these protons, as the chemical shift of C^{18}–H also seems to correlate with the electronegativity[7] of the substituent at C^3.

What effect does this torsional rocking have on the conformation of rifamycin S and how does this effect the antibiotic's enzyme inhibitory activity? The most likely conformational change, that pictured in Figure 6, tends to raise the stationary section of the ansa bridge up and out, exposing the C^{21}- and C^{23}-hydroxyl groups to a greater extent than in rifamycin S

Table II. Chemical Shifts for the Ansa Bridge Protons of 3-Substituted Rifamycin SV Derivatives[a]

SV-A	SV-NHR	SV-SR	SV-Cl	SV-Br	SV-I	SV-CN		SV-CN	SV-I	SV-Br	SV-Cl	SV-SR	SV-NHR	SV-A
11.91	8.91	9.93	8.45	8.55	8.49	8.22	H—N							
							C=O							
							C—CH_3	2.08	2.08	2.08	2.07	2.05	2.06	1.98
6.30	6.34	6.55	6.47	6.47	6.49	6.45	H—C							
10.7	11	11	11	10.7	10	11								
6.48	6.64	6.67	6.59	6.60	6.61	6.57	H—C							
15	15.3	14.8	14.6	15	15	14.5								
5.82	5.92	6.05	6.09	6.05	6.05	6.08	H—C							
4.9	4.2	4.9	5.2	4.9	4.4	5.3								
							H—C—CH_3	1.02	1.02	1.02	1.02	1.01	1.02	0.89
9.5	9.8	9.6	9.5	9.5	9.3	9.8								
3.67	3.83	3.82	3.92	3.94	3.94	3.92	H—C—OH	3.76	3.68	3.66	3.65	3.67	3.65	
							H—C—CH_3	0.94	0.90	0.89	0.88	0.90	0.84	0.78
2.93	3.04	3.03	3.04	3.03	3.04	3.03	H—C—OH	3.76	3.81	3.74	~3.7	3.79	3.73	
							H—C—CH_3	0.81	0.73	0.74	0.76	0.67	0.64	0.48
						1.3								
4.89	4.90	4.87	4.88	4.98	4.90	4.9	H—C—OAc	2.06	2.07	2.07	2.07	2.05	2.03	1.95
9.5	10.3	10.5	11	11	10	10.5								
							H—C—CH_3	−0.30	−0.29	−0.30	−0.30	−0.33	−0.29	−0.45
						1.5								
3.30	3.49	3.51	3.52	3.54	3.52	3.43	H—C—OMe	3.03	3.04	3.03	3.04	3.03	3.04	2.92
7.0	6.8	6.2	7.5	6.7	6.2	7.2								
5.01	5.09	5.06	5.09	5.09	5.10	5.08	H—C							
12.7	12.7	12.7	12.7	12.7	12.5	12.9								
6.12	6.22	6.14	6.25	6.21	6.15	6.22	H—C							
							O							

[a] Chemical shifts are listed on line with their respective protons in parts per million, while the respective coupling constants are listed between the coupled protons. Coupling constants for the $C^{21}H-C^{22}H$, $C^{22}H-C^{23}H$, $C^{23}H-C^{24}H$, and $C^{25}H-C^{26}H$ bonds were less than 0.5 Hz. The $C^{21}H$, $C^{23}H$, $C^{25}H$, and $C^{27}H$ protons appeared as slightly broadened doublets instead of the expected doublet of doublets.

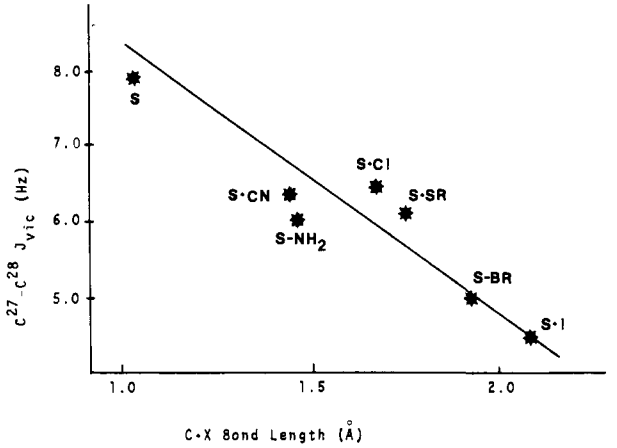

Figure 7. Correlation of $C^{27}H-C^{28}H$ coupling constants with C–X bond length (Å). Bond lengths used were (1) C–H, 1.05 Å; (2) C–N, 1.45 Å; (3) C–S, 1.73 Å; (4) C–Cl, 1.70 Å; (5) C–Br, 1.93 Å; (6) C–I, 2.09 Å; (7) C–C≡N, 1.40 Å.[8]

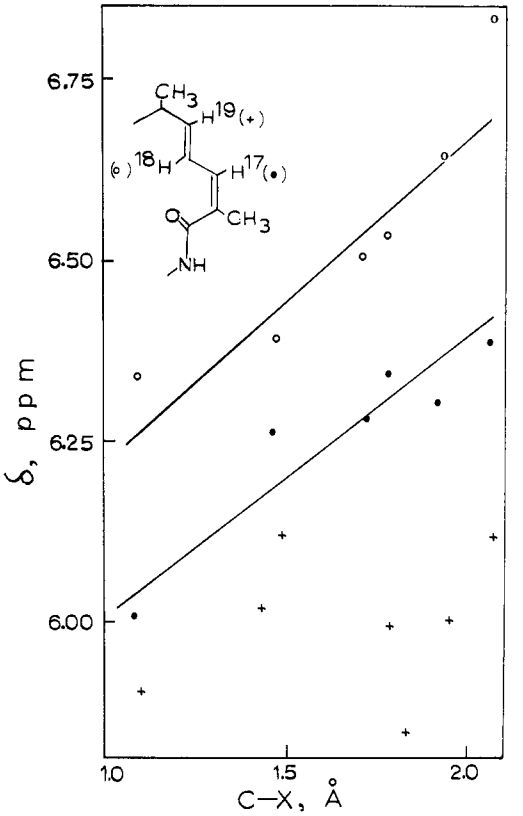

Figure 8. Chemical shift dependence of $C^{17}H$, $C^{18}H$, and $C^{19}H$ as a function of the C–X bond length.

itself, as the C^3 substituent increases in size. At the same time the amide-distal part of the ansa bridge collapses into the naphthalene ring with a concurrent upfield shift of the C^{34}-methyl. This change seems to follow the size of the C^3 substituent, at least in the halogen-substituted series. Although there are clearly electronegativity-dependent effects on the chemical shifts of the various ansa protons, our inability to separate ring current effects and amide carbonyl and C^3-substituent anisotropy effects in a molecule of this complexity makes conformational interpretation of these impossible.

We have previously shown[1] that whereas the RNA polymerase inhibitory activity of rifamycin S is quite dependent on the nature of the substituent at C^3, the analogous rifamycin SV derivatives are indistinguishable from one another. Particularly striking were the 3-amino derivatives. In rifamycin S these were almost devoid of inhibitory activity while in the case of rifamycin SV they are as active as rifamycin SV itself. That there are marked substituent effects on the conformations

of substituted rifamycin S but not SV derivatives suggests that the observed conformational changes are linked to enzymatic activity, perhaps in the sense of exposing the ansa hydroxyls as alluded to above. On the other hand, the conformational effects seem to parallel size of substituent while inhibitory effects parallel electronegativity. We are thus led to one of two possible conclusions.

(1) The observed conformational changes are unrelated to the question of enzymatic activity. This seems unlikely on the face of it but it could be that the only role of the ansa bridge is to afford a hydrophobic cross-ring bridge. Alternatively, the enzyme "fit" and conformational mobility of the ansa bridge could be such that minor changes in the latters' solution conformation can be tolerated without appreciable modification of the interaction between the enzyme and the ansa functionality.

(2) The observed conformational changes are indeed of prime importance in defining inhibitory activity, and the basic Karplus equation approach is too crude to pick out the rather subtle interplay between the steric and electronic effects of the substituents. In this respect we find it quite frustrating to be unable to translate the observed chemical shift changes into meaningful conformational changes. One could do this if one could assume a fixed geometry for all derivatives but this is demonstrably not the case. One can only note with a sense of wonderment that changing a chlorine to an iodine gives rise to, as its major effect, a twisting about a bond some ten atoms away! The present data are just too inexact to decide between these two alternatives.[9]

References and Notes

(1) H. W. Whitlock and M. F. Dampier, *J. Am. Chem. Soc.*, **97**, 6254 (1975).
(2) M. L. Casey and H. W. Whitlock, *J. Am. Chem. Soc.*, **97**, 6231 (1975).
(3) S. G. Gallo, E. Martinelli, V. Pagani, and P. Sensi, *Tetrahedron*, **30**, 3093 (1974).
(4) W. Kump and H. Bickel, *Helv. Chim. Acta*, **56**, 2323 (1973).
(5) M. Brufani, W. Fedeli, G. Giacomello, and A. Vaciago, *Experientia*, **20**, 339 (1964).
(6) J. Leitich, V. Prelog, and P. Sensi, *Experientia*, **23**, 505 (1967).
(7) R. C. Fort, Jr., and P. v. R. Schleyer, *J. Org. Chem.*, **30**, 789 (1965); F. W. van Deursen and P. K. Korver, *Tetrahedron Lett.*, **40**, 3923 (1967).
(8) "Handbook of Chemistry and Physics", 55th ed, CRC Press, Cleveland, Ohio, 1975.

(9) Support of this work by NIH is acknowledged.

Studies on the Mode of Action of the Mitomycin Antibiotics. Reversible Conversion of Mitomycin C into Sodium 7-Aminomitosane-9a-sulfonate

Ulfert Hornemann,* Yau-Kwan Ho, Jesse K. Mackey, Jr., and Suresh C. Srivastava

Contribution from the Department of Medicinal Chemistry and Pharmacognosy, School of Pharmacy and Pharmacal Sciences, Purdue University, West Lafayette, Indiana 47907.
Received March 8, 1976

Abstract: Reduction of mitomycin C with sodium dithionite in Tris buffer at 0 °C for a short period of time and subsequent reoxidation with oxygen gas yields 7-aminomitosane-9a-sodium sulfonate and red compounds of unknown structures. 7-Aminomitosane-9a-sodium sulfonate is also obtained at low temperature by catalytic reduction of mitomycin C over a palladium/charcoal catalyst in aqueous solution containing sodium sulfite and subsequent reoxidation. It can be converted back into the starting material by catalytic reduction at 0 °C in methanolic solution in the presence of sodium methoxide followed by reoxidation. These reactions constitute novel interconversions of mitosanes which may have a bearing on the formation of the naturally occurring mitomycin relative, mitiromycin. In addition, the formation of 7-aminomitosane-9a-sodium sulfonate suggests the possibility that C-9a of the mitomycins may be involved to some extent in the alkylation of biological macromolecules. 7-Aminomitosane-9a-sodium sulfonate is the first compound ever to be derived from any member of the mitomycins in a reduction–reoxidation sequence in aqueous solution. It is more stable in acidic medium than mitomycin C and like the parent antibiotic it shows antibacterial activity, albeit at a reduced level. The red compounds obtained show uv spectra similar to those of 7-aminoindoloquinones and they lack the carbamoyl group present in their precursor. The results of this investigation are considered to support, in part, proposals made by others on the mechanism of alkylation of biological macromolecules by mitomycin C.

It is well established that the mitomycin antibiotics[1,2] (I), which are elaborated by *Streptomyces verticillatus*[3] and by other strains of *Streptomyces*,[4] require reductive activation to become alkylating agents of biological macromolecules including DNA.[5] Bifunctional alkylation of the latter leading to the cross-linking of the two strands is considered to be an important feature in the mode of action of mitomycin C[6] and this bifunctional alkylation is presumably at least in part responsible for its effectiveness as an anticancer agent.[7,8]

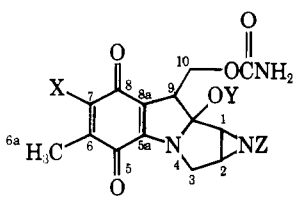

I

Ia, X = OCH_3; Y = CH_3; Z = H
b, X = OCH_3; Y = H; Z = CH_3
c, X = NH_2; Y = CH_3; Z = H

Studies have been undertaken in several laboratories to gain information on the mutual binding sites between mitomycin C and DNA but these binding sites have not been unambiguously identified. Szybalski and Iyer[9] introduced sodium dithionite as an efficient reducing reagent for in vitro studies and showed that reduced mitomycin C can react with DNA by monofunctional and bifunctional alkylation. These authors proposed that alkylation involved C-1 after opening of the aziridine ring and/or C-10 after displacement of the carbamoyl